

Improved Adaptive Control Algorithm of a Grid-Connected PMSG-Based Wind Energy Conversion System



Masood Nazir, Ikhtlaq Hussain, and Aijaz Ahmad

Abstract This paper investigates a permanent magnet synchronous generator (PMSG)-based wind energy conversion system (WECS) evaluating various conditions of power flow. The variable parameter reweighted zero-attracting least mean square (VP-RZA-LMS) algorithm is applied to the voltage source inverter (VSI) to account for a variety of power quality problems like compensation of reactive power, power balancing and active power transfer. A Simulink model is developed to validate the same. The proposed control algorithm provides faster convergence speed and is also dependent on a relatively lesser number of parameters.

Keywords Wind energy conversion system (WECS) · Permanent magnet synchronous generator (PMSG) · Power quality · Least mean square (LMS) · Power electronics

1 Introduction

Over the years, the topic of energy crisis has hogged the limelight partly due to the ever-increasing demand of electrical energy and partly due to the rapid extinction of non-renewable energy sources. The swell in pollution levels due to the exploitation of non-renewable energy sources coupled with the surge in the prices of traditional energy sources has compelled researchers to look for viable alternatives. Sustainable

M. Nazir (✉) · A. Ahmad

Department of Electrical Engineering, National Institute of Technology Srinagar, Srinagar, India
e-mail: masoodnazir111@gmail.com

A. Ahmad

e-mail: aijaz54@nitsri.net

I. Hussain

Department of Electrical Engineering, University of Kashmir, Zakura Campus, Srinagar, India
e-mail: ikhlaqiitd2015@gmail.com

energy sources, viz solar and wind, are an option in remote areas [1–4] where the cost of electricity by traditional means is a costly affair.

Although different types of generators with multiple converter topologies have been mentioned in the literature [5, 6], it has not been possible to completely penetrate the renewable energy sector yet. However, with proper government support in the form of national schemes and subsidies along with the advancement in power electronics [7], an effort is being made to take the renewable energy generation to the next level. The constant speed wind turbines use permanent magnet synchronous generators (PMSGs) to deliver power at a constant frequency. The advantage that a PMSG [8–11] generator provides over a regular induction generator is that there is no need of external excitation, and it is easier to control. Besides, it provides higher efficiency and reliability as well as its size is considerably small. Also, speed control is not required that is quite a task for variable speed wind turbines [12–14].

A lot of control algorithms have been devised for robust and reliable switching of the voltage source inverter (VSI) [15]. In this paper, the least mean square (LMS) algorithm is improved upon by including powerful adaptive filtering methods for system identification. Till date, several algorithms based on LMS have been proposed like proportionate normalized LMS (PNLMS), zero-attracting LMS (ZA-LMS) and resized zero-attracting LMS (RZA-LMS) [16]. Whereas the former repeatedly adjusts the step size that varies in accordance with the filter coefficient by updating it independently, the latter introduces variable step size strategy as the name suggests. Though ZA-LMS and RZA-LMS perform marginally better than LMS in varied situations, they are relatively tricky to implement because adjusting the step size is not easy.

In this paper, a permanent magnet brushless direct current (PMBLDC)-based wind energy conversion system (WECS) is suggested with a seamless variable parameter ZA-LMS (VP-ZA-LMS) control of VSI. The PMBLDC generator transforms the mechanical energy of wind into electrical energy which is fed to a diode bridge rectifier (DBR) for conversion from AC to DC. This power is fed at the DC bus of the converter by incorporating a boost converter that carries out the tracing of supremum power (MPPT). The advantages of the proposed control algorithm are:

- It provides faster convergence speed.
- This algorithm depends on lesser number of parameters that do not affect the system performance.

The proposed grid-tied WECS is simulated in MATLAB environment.

2 System Topology

A WECS is pictorially represented in Fig. 1. It consists of a wind turbine, PMSG machine and a DBR that is coupled to a converter. The wind energy source is connected at the DC bus of the converter to maintain a constant DC bus voltage. The wind turbine is coupled to a PMSG generator whose output is fed to a DBR. The DC

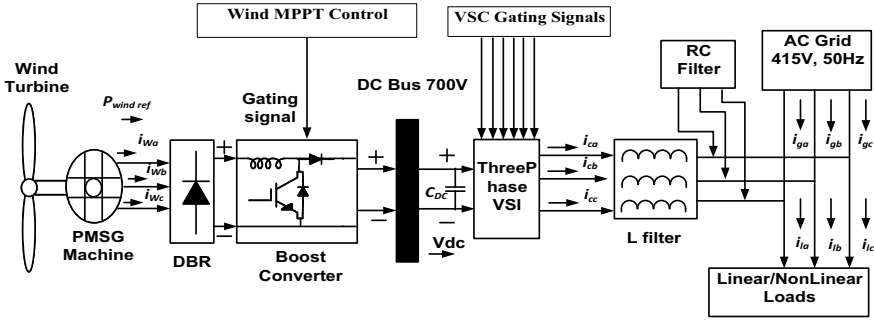


Fig. 1 System topology

power thus obtained is input to a boost converter that is responsible for MPPT. The system is operated in such a way so as to trace continuously its supremum point of power for maximum efficiency. For improvement of power quality and to account for harmonic suppressions, interfacing inductances and RC filter are connected at the point of common coupling (PCC).

3 Modeling and Design of WECS

Different components that comprise a WECS are a wind turbine, PMSG machine and a DBR that is coupled to a converter. The modeling of these components is described in this section.

3.1 Mathematical Model of Wind Turbine

The mechanical energy produced from wind is a function of wind speed [2]. It is given as

$$P_w = \frac{1}{2} \rho A C_p(\lambda, \beta) v^3 \tag{1}$$

$$\lambda = w_m \frac{R}{v} \tag{2}$$

$$C_p = C_1 \left(\frac{C_2}{\gamma} - C_3 \beta - C_4 \right) e^{\frac{C_5}{\gamma}} + C_6 \gamma \tag{3}$$

where ρ = air density, v = wind speed (m/s), A = area swept by the rotor, C_p = power coefficient, β = pitch angle and R = rotor radius. The wind turbine torque is given as

$$T_m = \frac{P_m}{w_m} \quad (4)$$

The largest value of C_p is $C_{p\max} = 0.48$ and is obtained for pitch angle = 0 and $\lambda = 8.1$ so that the power extracted is maximum and is given by

$$P_{\max} = \frac{1}{2} \rho A C_P \frac{R^3}{\lambda_{\text{opt}}^3} w_m^3 \quad (5)$$

3.2 Modeling of PMSG

A PMSG machine of power rating 3.7 kW with the winding resistance of stator as R_{st} , stator flux ($\psi_{f_{sd}}, \psi_{f_{sq}}$), direct and quadrature axis stator inductances as (L_{sd}, L_{sq}), PM flux linkage as ψ_{pm} , n number of pole pairs and dq axis voltages and currents of stator as V_{sdq}, i_{sdq} coupled with a 10kW wind turbine comprises a WECS. The mathematical equations are expressed as [14]

$$V_{sd} = -R_{st}i_{sd} - p\psi_{f_{sd}} + nw_m\psi_{f_{sq}} \quad (6)$$

$$V_{sq} = -R_{st}i_{sq} - p\psi_{f_{sq}} - nw_m\psi_{f_{sd}} \quad (7)$$

$$\psi_{f_{sd}} = L_{sd}i_{sd} + \psi_{pm} \quad (8)$$

$$\psi_{f_{sq}} = L_{sq}i_{sq} \quad (9)$$

3.3 Boost Converter Calculations

The duty cycle (D) and the values of capacitor and inductor of the boost converter are calculated as [15]:

$$V_{\text{out}} = \frac{V_{\text{in}}}{1 - D} \quad (10)$$

$$L = V_{\text{in}} \frac{V_{\text{out}} - V_{\text{in}}}{i_{\text{ripple}}} f_s V_{\text{out}} \quad (11)$$

$$C = I_{\text{out}} \frac{D}{\delta V f_s} \quad (12)$$

where f_s is 10 kHz, V_{in} is the voltage input to boost converter, V_{out} is the equivalent DC bus voltage and δV is the acceptable voltage distortion content chosen as 1–2% of V_{out} .

3.4 Design of VSC

A three-legged VSC that is meant for compensating reactive power in the system comprises six IGBTs, three AC inductors and a DC capacitor. It is designed for a 415 V, 50Hz system [15].

3.5 Design of Interfacing Inductance and RC Filter

An RC filter is used to refine the voltage at the point of common coupling (PCC) by draining out noise from it. Considering $R_f C_f = T_s/10$ and switching frequency equal to 2 kHz, the specifications of ripple filter are calculated as $R_f = 10 \Omega$ and $C_f = 10 \mu\text{F}$, where R_f , C_f are the resistance and capacitance of the ripple filter and T_s is the switching time [15]. The value of interfacing inductance is taken as 5.5 mH [15].

3.6 Scheme of DC Link Capacitor and DC Bus Voltage

DC link capacitance is calculated as [15]

$$\frac{1}{2} C_{DC} (V_{DC}^2 - V_{DC1}^2) = k3VmIt \quad (13)$$

where V_{DC} is the reference DC voltage and V_{DC1} is the minimum voltage level of the DC bus, m is the overloading factor, V is the phase voltage, I is the phase current and t is the time by which the DC bus voltage is to be recovered. The value of DC link capacitance thus calculated is 10,000 μF .

The least value of DC bus voltage needs to be higher than two times the phase voltage peak. It is calculated as

$$V_{DC} = \frac{2\sqrt{2}V_{LL}}{\sqrt{3}p} \quad (14)$$

where p is the modulation index=1 and V_{LL} is the line to line output voltage. V_{DC} thus obtained is 677.7 V for a line voltage of 415 V and is rounded off as 700V.

4 Control Algorithm

The system is handled by regulating the DC current of the circuit in such a way such that the point corresponding to supremum power (MPP) is traced continuously. The control algorithm consists of wind control and VSC control which are mentioned in the following section.

4.1 Wind Generator Boost Converter Control

The control, shown in Fig. 2, uses a PI controller which reduces the error between the desired current and the actual DC current to zero and in the process draws out maximum generator power. The PI controller input is an error signal that is generated as

$$I_{wind, err} = \frac{P_{wind, ref}}{v_{windDC}} \tag{15}$$

The boost converter utilizes this error signal input to a PI controller to control the output DC current and power.

4.2 Control Algorithm for VSC

In this paper, a VP-RZA-LMS algorithm [16] as shown in Fig. 3 is proposed where the parameters like step size are repeatedly adjusted. This method keeps on minimizing the mean square error (MSE) and converges relatively faster. The simulation results further validate the performance of the algorithm. Initially, the unit template components are calculated as [15]:

$$\mu_{pa} = \frac{v_{sa}}{v_t}; \mu_{pb} = \frac{v_{sb}}{v_t}; \mu_{pc} = \frac{v_{sc}}{v_t} \tag{16}$$

Voltage at PCC is given by

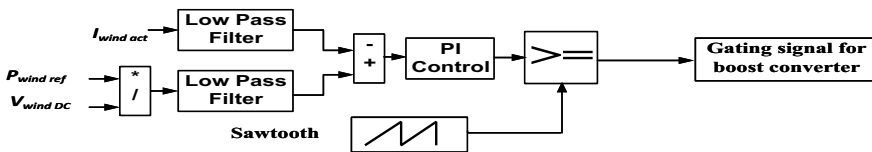


Fig. 2 Wind MPPT control algorithm

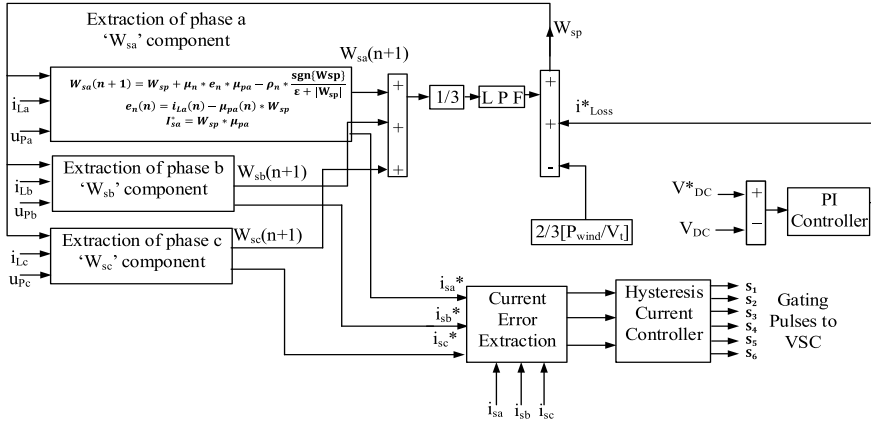


Fig. 3 Proposed control algorithm for VSC

$$V_t = \sqrt{2/3(v_{sa}^2 + v_{sb}^2 + v_{sc}^2)} \tag{17}$$

Next, the corresponding error is obtained by utilizing the unit templates as shown in

$$e_n = i_{La} - \mu_{pa} W_{sp} \tag{18}$$

The RZA-LMS update is obtained by using stochastic subgradient iterations and is given by

$$W(n + 1) = W_n + \mu e_n w_n - \rho \frac{\text{sgn}[W_n]}{\epsilon + |W_n|} \tag{19}$$

where the absolute value operator is applied in an element-wise manner and ϵ is a small positive parameter. The parameter w_n is initialized as $w_n = 0.01$.

The active weight components for the three phases are estimated by subtracting w_n from the above equation and subsequently substituting (18) in it. The active weight components are given by equations (20), (21) and (22)

$$W_{sa}(n + 1) = W_{sp} + \mu_n e_n \mu_{pa} - \rho_n \frac{\text{sgn}[W_{sp}]}{\epsilon + |W_{sp}|} \tag{20}$$

$$W_{sb}(n + 1) = W_{sp} + \mu_n e_n \mu_{pb} - \rho_n \frac{\text{sgn}[W_{sp}]}{\epsilon + |W_{sp}|} \tag{21}$$

$$W_{sc}(n + 1) = W_{sp} + \mu_n e_n \mu_{pc} - \rho_n \frac{\text{sgn}[W_{sp}]}{\epsilon + |W_{sp}|} \tag{22}$$

Adding Eqs. (20), (21) and (22), the mean value of the fundamental active component is given as

$$W_p = \frac{1}{3}(W_{sa} + W_{sb} + W_{sc}) \quad (23)$$

The reference supply currents for the three phases are calculated as

$$i_{sa}^* = W_{sp} * \mu_{pa}; i_{sb}^* = W_{sp} * \mu_{pb}; i_{sc}^* = W_{sp} * \mu_{pc} \quad (24)$$

5 System Performance

The proposed system consists of a 10kW wind turbine that is coupled to a 3.7kW PMSG machine. The output is fed to a bridge rectifier via a boost converter. The VSC feeds power to linear/nonlinear loads. The source voltage is 415 V at 50Hz. The system is operated under steady-state and dynamic conditions by varying wind speed and incorporating load unbalancing conditions. A Simulink model is designed to validate the results in detail.

5.1 Steady-State Performance Under Nonlinear Load

The conduct of a grid-tied WECS evaluated on the application of a nonlinear load is shown in Fig. 4. It shows the waveforms of source voltage v_{abc} , source current i_{abc} , load current i_{Labc} , converter current i_{vsc} , DC bus voltage v_{DC} , wind velocity v_{wind} , wind current i_{wind} and wind power p_{wind} . It is clear that when the load current (2 A) is less than the converter current (5 A), the wind source supplies power to both load as well as grid. However, when the load current exceeds the converter current, the grid supplies power to both load as well as the wind source.

5.2 Steady-State Performance Under Linear Load

Figure. 5 shows the behavior of a grid-tied WECS evaluated on the application of a linear load. It depicts the waveforms of source voltage v_{abc} , source current i_{abc} , load current i_{Labc} , converter current i_{vsc} , DC bus voltage v_{DC} , wind velocity v_{wind} , wind current i_{wind} and wind power p_{wind} .

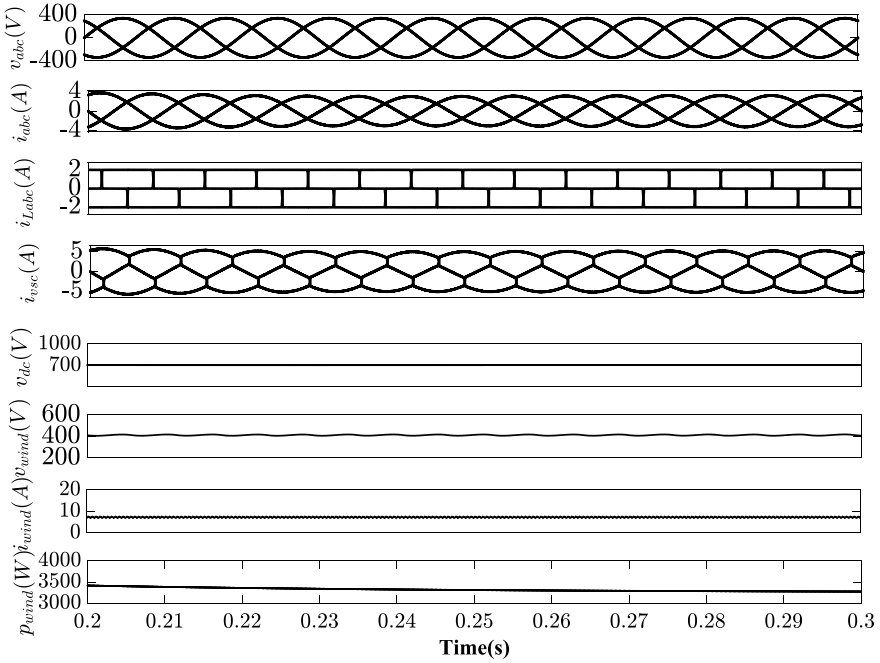


Fig. 4 Steady-state performance under nonlinear load when i_{load} is less than i_{vsc}

Figure 5a depicts that when the load current is less than the converter current, wind supplies power to both load and grid. However, when the load current is greater than converter current as shown in Fig. 5b, grid supplies power to both load and wind energy source.

5.3 Dynamic Performance Under Nonlinear Load

Figure 6 shows the behavior of a grid-tied WECS evaluated on the application of a nonlinear load. It depicts the waveforms of source voltage v_{abc} , source current i_{abc} , load current i_{Labc} , converter current i_{vsc} , DC bus voltage v_{DC} , wind velocity v_{wind} , wind current i_{wind} and wind power p_{wind} . It is observed that at time $t = 0.5$ s, phase B of the load is reconnected to the system, but grid current remains sinusoidal and balanced. It is also observed that DC link voltage is maintained close to reference value under all disturbances.

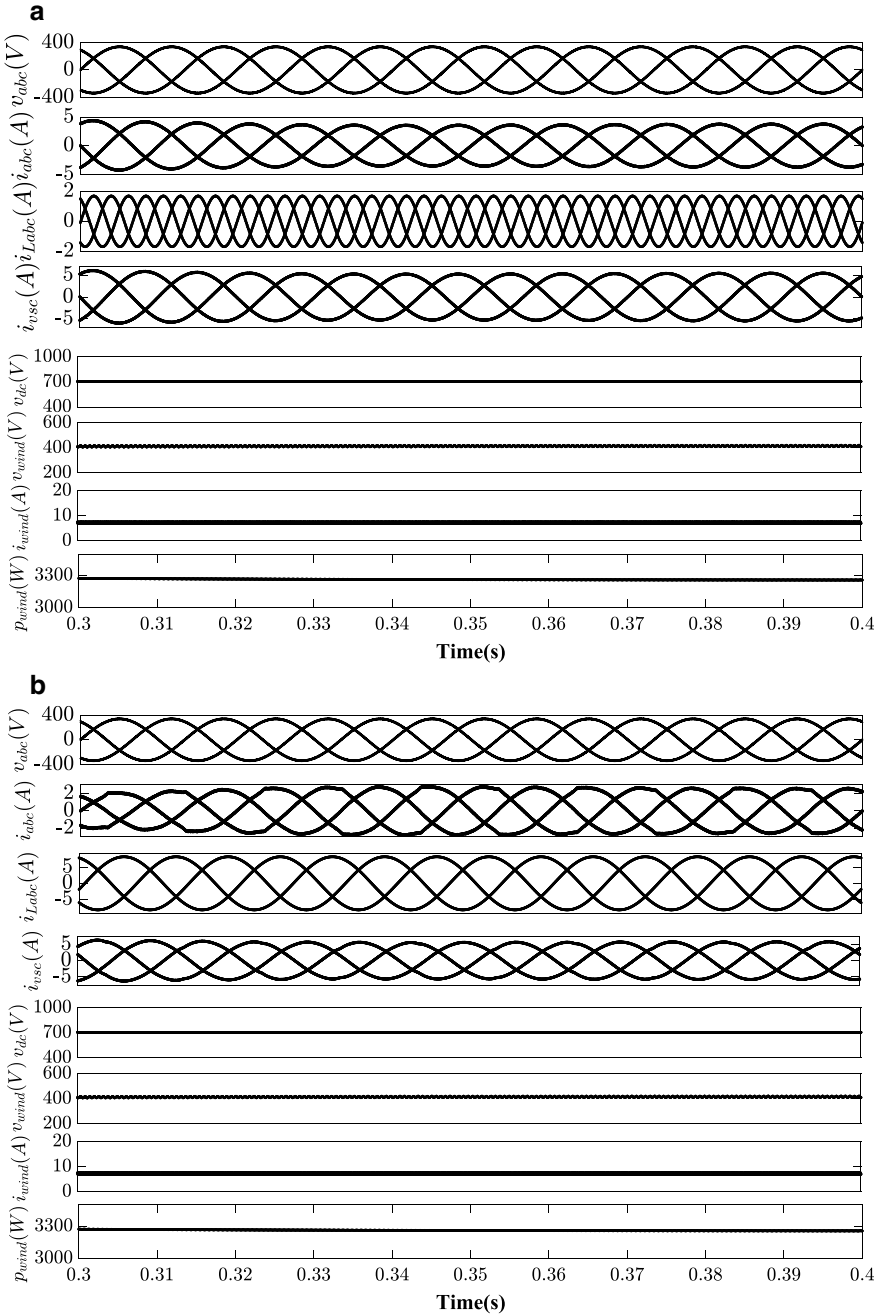


Fig. 5 **a** Steady-state performance under linear load when i_{load} is less than i_{vsc} , **b** steady-state performance under linear load when i_{load} is greater than i_{vsc}

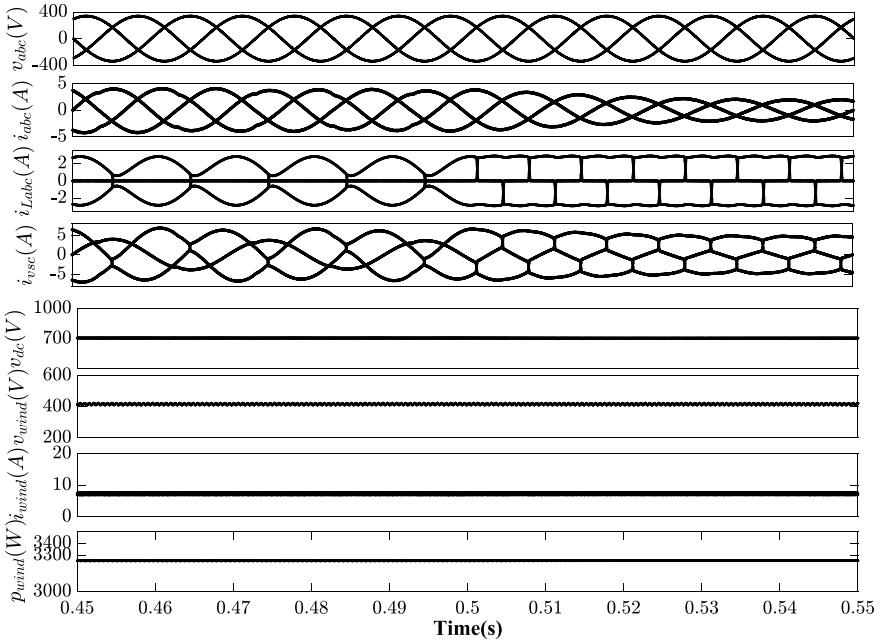


Fig. 6 Dynamic performance under a nonlinear load

5.4 Dynamic Performance Under Nonlinear Load Due to Change in Wind speed

The dynamic performance under a nonlinear load due to change in wind speed is shown in Fig. 7. It shows the waveforms of source voltage v_{abc} , source current i_{abc} , load current i_{Labc} , converter current i_{vsc} , DC bus voltage v_{DC} , wind velocity v_{wind} , wind current i_{wind} , wind power p_{wind} , wind speed v (m/s), rotor speed v_r and torque T_m . It is observed from the figure that wind power is close to 3400 W at a wind speed of 12 m/s, and wind source supplies power to the load. However, at $t = 0.5$ s to $t = 1$ s, when the wind speed is reduced from 12 to 7 m/s, it is observed that the wind power reduces from 3400 to 1500 W. Under such conditions, the wind source is unable to supply power to the load which is evident from the waveforms of Fig. 7. Under such conditions, grid supplies power to the load.

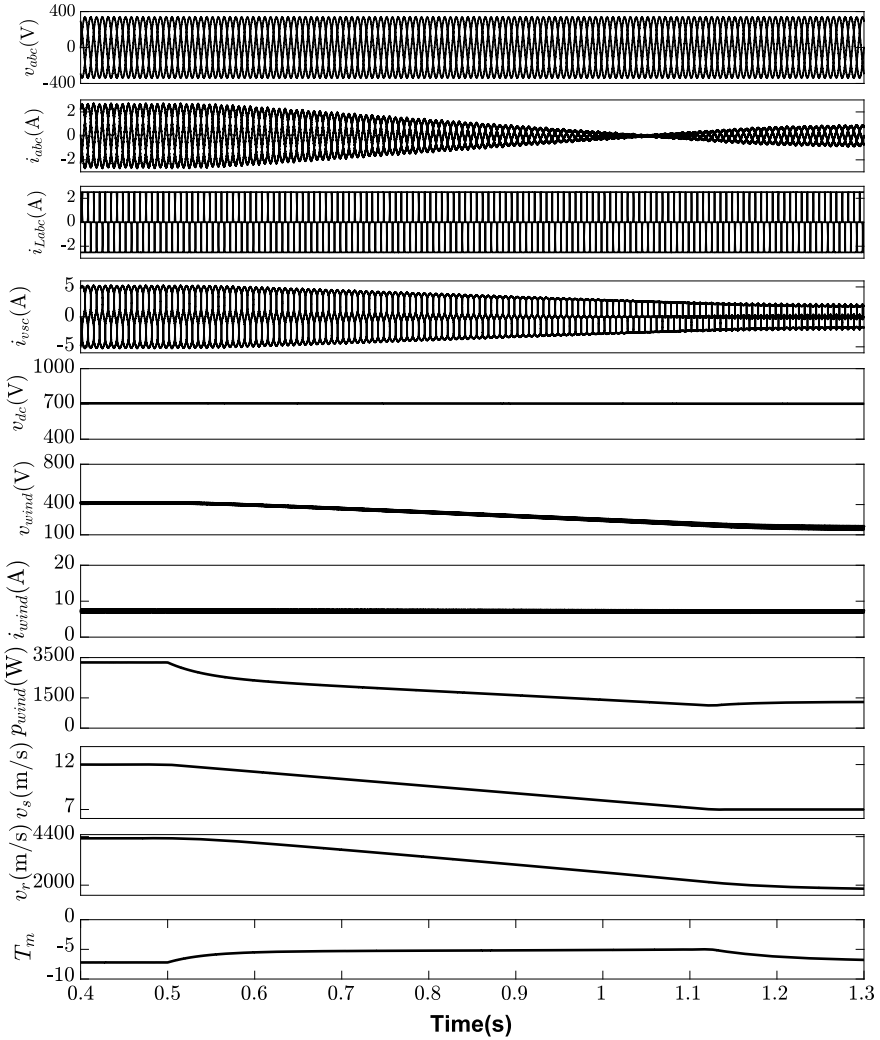


Fig. 7 Dynamic performance under nonlinear load due to wind speed variation

6 Conclusions

The performance of a grid-integrated WECS has been carried out in SIMULINK. The PMSG transforms the mechanical energy of the wind into electrical energy which has been rectified and conditioned and finally fed to the grid. Adaptive control of WECS is incorporated by implementing VP-RZA-LMS algorithm to provide power quality solutions like power balancing, active power transfer and voltage regulation.

Also, favorable results have been obtained under changing wind speeds. Such a setup is very much capable of providing an able backup in remote locations.

Appendix

Wind Turbine: Cut in wind speed = 6 m/s, rated wind speed = 12 m/s, $C_{pmax} = 0.48$, $\lambda_{TSR} = 8.1$, $C_1 = 0.5175$, $C_2 = 116$, $C_3 = 0.4$, $C_4 = 5$, $C_5 = 21$, $C_6 = 0.0069$,
PMSG Rating: 5 hp, 230 V, $n = 4$, $R_s = 1.785 \Omega$, Stator Phase Inductance = 9.065 mH
System Parameters: Boost converter inductance, $L_b = 10$ mH, DC link capacitance, $C_{dc} = 10,000 \mu\text{F}$, $K_p = 1$, $K_i = 0$, $V_{dc} = 700$ V, Adaptive filter constant, $\mu_n = 0.01$, $\rho_n = 0.006$, $\epsilon = 0.002$.
Interfacing inductance, $L_{int} = 5$ mH, 3 phase grid voltage, $V_{abc} = 415$ V (rms), $R_f = 10 \Omega$, $C_f = 10 \mu\text{F}$, Sampling time, $T_s = 10 \mu\text{s}$.

References

1. Pimentel D (2008) Biofuels, solar and wind as renewable energy system-benefits and risks. Springer, Colorado
2. Wu B, Lang Y, Zargari N, Kouro S (2011) Power conversion and control of wind energy systems, Wiley, Inc., Hoboken, New Jersey
3. Rashid A, Hasan N, Parvez KT, Maruf (2015) MNI Study and analysis of a small-scale micro-grid using renewable energy resources. In: Proceedings of international conference on electrical engineering and information communication technology (ICEEICT). Dhaka, pp 1–4
4. Lasseter RH (2011) Smart distribution: coupled microgrids. Proc IEEE 99(6):10/4-1082
5. Yahia H, Liouane N, Dhifaoui R (2014) Differential evolution method based output power optimisation of switched reluctance generator for wind turbine applications. IET Renew Power Gener 8(7):795–806 September
6. Rezaei E, Ebrahimi M, Tabesh A Control of DFIG wind power generators in unbalanced microgrids based on instantaneous power theory. IEEE Trans Smart Grid PP(99):1–8
7. Mulholland R, McBride V, Vial C, O'Malley A, Bennett D (2015) 2015 top markets report renewable energy. <http://www.trade.gov/industry>
8. Sun L, Gong C, Han F (2013) Design and optimization of control parameters based on direct-drive permanent magnet synchronous generator for wind power system. In: Proceedings in 8th IEEE conference on industrial electronics and applications (ICIEA). VIC, Melbourne, pp 1238–1243
9. Haque ME, Muttaqi KM, Negnevitsky M (2008) Control of a stand alone variable speed wind turbine with a permanent magnet synchronous generator. In: Proceedings in IEEE power and energy society general meeting—conversion and delivery of electrical energy in the 21st century. Pittsburgh, PA, pp 1–9
10. Pradhan S, Murshid S, Singh B, Panigrahi BK (2018) A robust SMOC for vector controlled PMSG based isolated wind energy generating system. In: IEEE industry applications society annual meeting (IAS). Portland, OR, pp 1–8
11. Pradhan S, Singh B, Panigrahi BK, Murshid S (2019) A composite sliding mode controller for wind power extraction in remotely located solar PV-wind hybrid system. IEEE Trans Ind Electron 66(7):5321–5331 July

12. Singh B, Panigrahi BK, Pathak G (2016) Control of wind-solar microgrid for rural electrification. In: IEEE 7th Power India international conference (PIICON). Bikaner, pp 1–5
13. Mishra S, Hussain I, Pathak G, Singh B (2018) dPLL-based control of a hybrid wind-solar grid connected inverter in the distribution system. *IET Power Electron* 11(5):952–960
14. Pathak G, Singh B, Panigrahi BK, Chandra A, Al-Haddad K (2016) Wind-PV based microgrid and its synchronization with utility grid. In: 2016 IEEE international conference on power electronics, drives and energy systems (PEDES). Trivandrum, pp 1–6
15. Singh B, Chandra A, Al-Haddad K (2014) *Power quality: problems and mitigation techniques*. Wiley
16. Jin D, Chen J, Richard C, Chen Jingdong (2018) Model driven online parameter adjustment for zero attracting LMS. *Signal Process* 152:373–383